Exploring the Dynamics of a Vibro-Impact Capsule Moving on the Small Intestine using Finite Element Analysis

Jiyuan Tian[1], Yang Liu[1], and Shyam Prasad[2]

[1] College of Engineering, Mathematics and Physical Sciences, University of Exeter, North Park Road, Exeter, EX4 4QF, UK,
y.liu2@exeter.ac.uk,
WWW home page: http://blogs.exeter.ac.uk/adce/
[2] Royal Devon and Exeter NHS Foundation Trust, Barrack Road, Exeter, EX2 5DW, UK

Abstract. This paper aims to study a realistic finite element (FE) model to depict the nonlinear dynamics of a vibro-impact capsule moving on the small intestine for active capsule endoscopy. The FE model takes both the nonlinear vibro-impact mechanism and the viscoelastic deformation of the small intestine into account. FE results are compared with the simulation results obtained using non-smooth differential equations and experimental results. It is found that the FE model can provide a more realistic prediction of the system in the complex intestinal environment in terms of capsule's tilted motion and asymmetric distribution of capsule-intestine contact pressure. In particular, the capsule's dynamics is very sensitive to the surface condition of the intestine, so a comprehensive bifurcation analysis is needed for fully understanding its dynamics under intestinal peristalsis.

Keywords: finite element, vibro-impact, stick-slip, friction, non-smooth dynamical system, capsule endoscopy

1 Introduction

Since its introduction into clinical practice two decades ago, capsule endoscopy has become established as the primary modality for examining the surface lining of the small intestine, an anatomical site previously considered to be inaccessible to clinicians. However, its reliance on peristalsis for passage through the intestine leads to significant limitations, in particular due to the unpredictable and variable locomotion speeds. Significant abnormalities may be missed, due to intermittent high transit speeds that lead to incomplete visualisation of the intestinal surface. Furthermore, each case produces up to 100,000 still images, from which video footage is generated, taking between 30 and 90 minutes for the clinician to examine in its entirety. The procedure is therefore considered both time-consuming and burdensome for clinicians. There is, therefore, in gastrointestinal (GI) endoscopic practice a desperate need for new modalities that are

safe, painless, accurate and reliable, which require minimal training for practitioners.

Leveraging their pioneering work in the field of controllable capsule endoscopy, the Applied Dynamics and Control Lab at the University of Exeter has developed a novel untethered, self-propelled, endoscopic capsule [1], with the aim of enabling cost effective small-bowel examination. Design innovations include self-propulsion for mobility and visualisation, facilitated manipulation, real-time screening, and short examination time. Building upon their successful pilot studies, including capsule-bowel contact modelling [2], experimental and numerical studies of intestinal frictions [3], capsule dynamics in the bowel environment [4], and their proof-of-concept validations [5, 6], with this further research the present work will study the dynamic response of the vibro-impact capsule when it moves in the intestinal environment with the consideration of tissue's mechanical properties by using finite element (FE) methods. This model can be then utilised to describe the detailed locomotion of the capsule and capsule-intestine interaction under vibro-impact dynamics.

The principle of the vibro-impact self-propulsion technique is that, the rectilinear motion of the capsule can be obtained using a periodically driven inner mass interacting with the main capsule body in the presence of environmental resistance [7]. The merit of such a system is its simplicity in mechanical design and control which does not require any external driving accessories, while allowing independent movement in a complex environment unaccessible to legged and wheeled robots [8]. Imagine for example, a miniaturised vibro-impact capsule which is moving inside the small intestine by adopting this method. In this case, many complications induced by external driving accessories, e.g. [9], can be avoided. However, understanding of the dynamics and efficient control of such a driving mechanism are critical, and researchers have been working on the modelling [10, 11], bifurcation analysis [12], and proof-of-concept verification [13]. So, it is worth developing this technique further and study its complex dynamics in a real intestinal environment by considering the intestinal anatomy and its mechanical properties, such as the viscoelasticity, the hoop stress and the haustral folds of the intestine.

In this paper, a new FE model of capsule-intestine contact coupling with the vibro-impact mechanism in the capsule was studied. Material properties of the intestinal tissue (e.g. viscoelasticity) and the geometry of the capsule (e.g. the arced shape) were considered in the model. The dynamic response of the capsule and the capsule-intestine interaction were studied through FE analysis in order to complement the insufficient consideration of environmental influence in the previous models [10, 12]. Some new phenomena of the capsule were observed which were not discovered in the literature before. The rest of the paper is organised as follows. In Section 2, FE modelling of the vibro-impact capsule moving on the small intestine is studied. A brief introduction of the experimental apparatus and procedure is provided in Section 3. In Section 4, FE results are compared with the simulation and the experimental results. Finally, conclusions are drawn in Section 5.

2 Finite element modelling

In this section, the material properties, the geometry, and the boundary conditions of the capsule and the small intestine are elaborated. The FE model was developed using ANSYS WORKBENCH Transient Structural module for which an implicit dynamics was applied.

2.1 Material properties

Since it fits better with our stress relaxation experiment [2], the three-element Maxwell model which contains two elastic springs and one viscous dashpot was adopted to describe the viscoelasticity of the synthetic small intestine. The three-element Maxwell model can expressed as

$$E(t) = E_1 e^{-\frac{E_1}{\eta_1}t} + E_2, \tag{1}$$

where E_1, E_2 and η_1 are the Young's moduli of the springs and the damping coefficient, respectively. In order to compare different supporting substrates for the capsule, aluminium bench was also tested in the FE model. Table 1 summarises all the parameters used in the FE model, where E and η are the Young's moduli, ρ is the material density, ν is the Poisson's ratio, μ is the friction coefficient, and the subscripts "c", "a", "s" and "i" represent the capsule, the aluminium bench, the inner mass and the intestine, respectively.

Table 1. Material properties of the FE model obtained from [2, 3].

Parameters	Values	Units	Parameters	Values	Units
E_c	0.11	GPa	ρ_c	0.95	$\mathrm{g \cdot mm^{-3}}$
E_a	71	GPa	ρ_a	2.77	$\mathrm{g \cdot mm^{-3}}$
E_s	200	GPa	ρ_s	7.85	$\mathrm{g \cdot mm^{-3}}$
E_i	25	kPa	ρ_i	1	$\mathrm{g \cdot mm^{-3}}$
E_1	196.43	kPa	ν_c	0.42	-
E_2	757.48	kPa	ν_a	0.33	-
η_1	5.36	MPa	ν_s	0.3	-
μ_a	0.3117	-	ν_i	0.49	-
μ_i	0.2293	-			

2.2 Model description and hypothesises

The 3D conceptual design of the capsule prototype is presented in Fig. 1(a), where the capsule has a primary and a secondary impact constraints and a linear bearing. The linear bearing holds a T-shaped magnet (inner mass), and restricts its motion in the axial direction of the capsule. The magnet is controlled by an external magnetic field excited by a pulse-width modulation signal. A helical spring connecting the magnet and the bearing was used to push the magnet back to its original position after each external excitation. The two impact constraints

restrict the axial motion of the magnet within a limited distance but magnify the excitation force through the vibro-impact dynamics. Due to the nonlinear characteristics of the small intestine and the nonlinear nature of the capsule system, computing a 3D FE model is time-consuming. So, the 2D FE model shown in Fig. 1(b) was developed, and the following hypothesises were introduced.

1. The stress of the 2D plane along the Z axis of the 3D model is zero.
2. The primary and the secondary constraints in the 3D model were replaced using the springs connecting with two rigid plates in the 2D model.
3. The inner mass only can move in the axial direction of the capsule along the frictionless bearing.

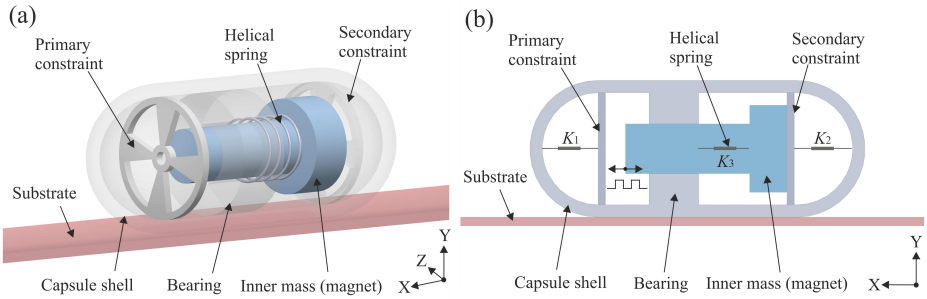

Fig. 1. (a) 3D conceptual design and (b) 2D FE model of the vibro-impact capsule moving on a cut-open small intestine.

Table 2. Physical parameters for the FE model obtained from [1].

Parameters	Values	Units	Parameters	Values	Units
M_1	1.80	g	M_2	1.67	g
K_1	14.24	$\mathrm{N \cdot mm^{-1}}$	C_1	0.01	$\mathrm{Ns \cdot m^{-1}}$
K_2	97.06	$\mathrm{N \cdot mm^{-1}}$	C_2	0.35	$\mathrm{Ns \cdot m^{-1}}$
K_3	0.06	$\mathrm{N \cdot mm^{-1}}$	C_3	0.01	$\mathrm{Ns \cdot m^{-1}}$

All the identified parameters of the 2D FE model were listed in Table 2, where M_1 and M_2 are the weights of the magnet and the capsule, K_1, K_2 and K_3 are the stiffness, C_1, C_2 and C_3 are the damping coefficients of the primary constraint, the secondary constraint and the helical springs, respectively.

2.3 FE setup and mesh convergence test

The dimension of the FE model is presented in Fig. 2(a), where the total length, the diameter and the thickness of the capsule are 26 mm, 11 mm and 1 mm, respectively. The total weight of the capsule is 3.47 g, including the capsule 1.67 g and the inner mass (magnet) 1.8 g. The thickness of the small intestine is 0.69 mm measured from the synthetic small intestine used in [3]. In order to consider the energy loss by the collisions between the inner mass and the primary and

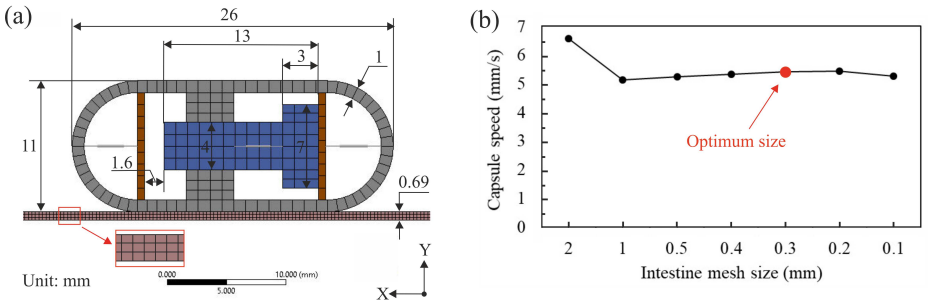

Fig. 2. (a) Dimension of the FE model and (b) mesh convergence tests: the capsule moving on the intestine at the excitation frequency 30 Hz, the duty cycle 80% and the excitation amplitude 6.8 mN. Red dot marks the chosen mesh size for the intestine.

the secondary constraints, they were set as quasi-rigid bodies in the FE model, so the primary spring K_1 and the secondary spring K_2 were more accurate to represent the constraints in the 3D model. The contact pair between the capsule and the substrate was set as frictional with their corresponding coefficients listed in Table 1. In order to get a more accurate simulation, the capsule-intestine contact algorithm was configured as Pure penalty, the normal contact stiffness factor was set as 1, and the sliding motion between the internal mass and the bearing was frictionless.

Due to the requirement of deformation, two types of elements were used to mesh the proposed model. The 4-node plane element (PLANE182) was used for modelling the capsule, the inner mass and the aluminum bench. The higher-order 8-node plane element (PLANE183) that exhibits quadratic displacement behavior was used to simulate the viscoelasticity of the intestine. Convergence tests using different mesh sizes were implemented, and their results were summarised in Fig. 2(b). It can be seen from the movement speed of the capsule that when the small intestine mesh is less than 1 mm, the FE result tends to converge. In order to obtain the best performance for the FE model, the mesh sizes for the capsule and the small intestine were set to 1 mm and 0.3 mm, respectively, and three-layer small intestine mesh was considered as presented in Fig. 2(a). For the boundary condition of the FE model, the substrates were fixed on the bottom surface. For the first 0.3 seconds of the simulation, the standard gravity was applied to the capsule, and the external excitation was applied to the inner mass after the capsule settled down along the Y axis.

3 Experimental apparatus and procedure

The prototype of the vibro-impact capsule is presented in the left panels of Fig. 3, and its experimental rig is shown in the right panel. The magnet inside the capsule was excited through an on-off electromagnetic field $\vec{B}$ and the helical spring to generate forward and backward impact motion, leading to the locomotion of the prototype. The on-off external excitation was generated using a signal gen-

erator producing a pulse-width-modulation signal via a power amplifier, and the amplifier can control the voltage applied to the coil by adjusting a DC power supply. The prototype was put on a piece of cut-open synthetic small intestine supported by a halved black plastic tube, which was placed along the axis centre of the coil. On the top of the experimental setup, a video camera was used to record the motion of the capsule, and recorded videos were analysed by using an open source software to generate the time history of capsule's displacement and velocity. A detailed experimental study and identification of the physical parameters can be found from [1].

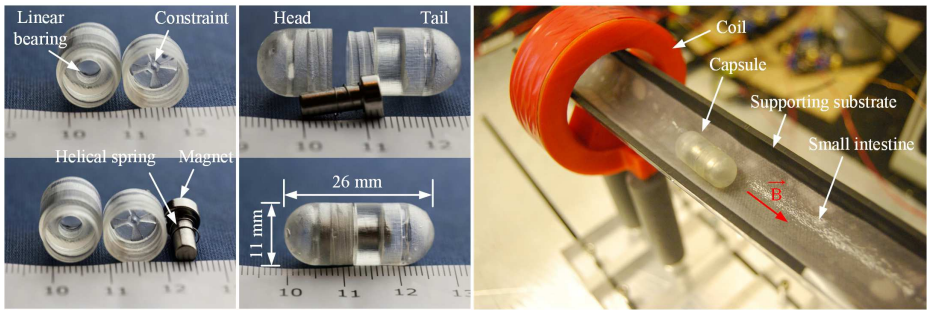

Fig. 3. [1] Left panels: Components and dimension of the prototype. Right panel: Photograph of the experimental setup.

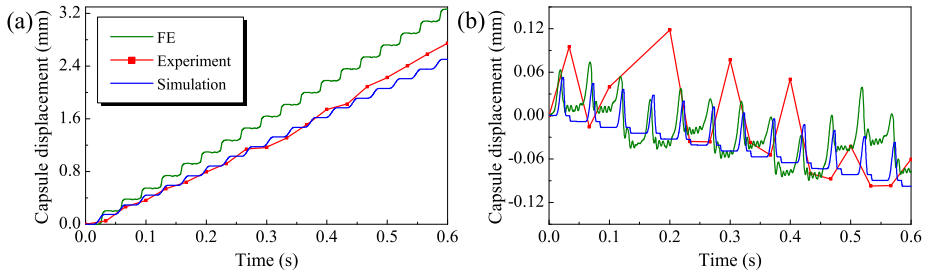

Fig. 4. (a) Time histories of capsule's displacements in X axis obtained at the excitation frequency 30 Hz, the amplitude 6.8 mN, and the duty cycle 0.8. (b) Time histories of capsule's displacements in X axis obtained at the excitation frequency 20 Hz, the amplitude 5.8 mN, and the duty cycle 0.3.

4 Results and analysis

FE results for the capsule moving on the small intestine are compared with the simulation obtained using MATLAB and experimental results [1] in Fig. 4. It can be seen that both forward and backward progressions are in good agreement. In Fig. 4(a), the progression speed of the capsule obtained from FE simulation is slightly higher than the other two results, which might be due to the experimental

inaccuracy in measuring the friction coefficient between the capsule and the intestinal surface. In Fig. 4(b), backward progression of the capsule was recorded, but it was a chaotic motion in FE and experiment while was a periodic motion in simulation. This reveals that the FE model is more realistic than the simulation model in terms of the asymmetries caused by the impact constraint and the capsule-intestine contact.

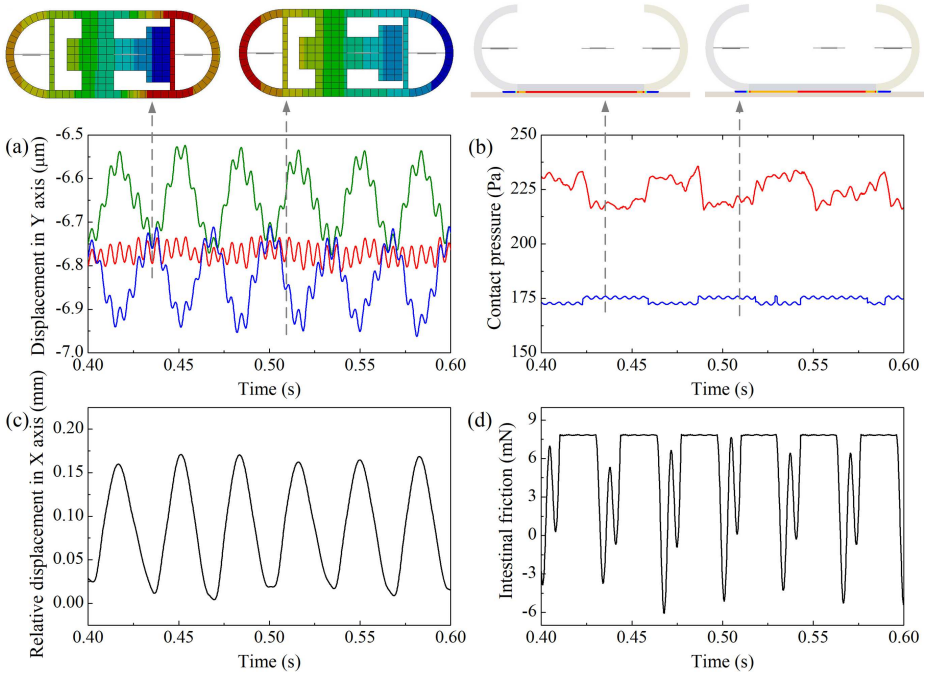

Fig. 5. (a) FE time histories of capsule's displacements in Y axis measured at the front (green line), middle (red line) and back (blue line) of the capsule, (b) capsule-intestine maximum (red line) and average (blue line) contact pressures, (c) magnet-capsule relative displacement and (d) intestinal friction obtained at the excitation frequency 30 Hz, the amplitude 6.8 mN, and The duty cycle 0.8. Extra panels in (a) present the contour map of displacement of the capsule in Y axis, where red and blue colours denote large and small displacement, respectively. Extra panels in (b) present the contour map of pressure distribution on the small intestine, where red and blue colours represent high and low pressure, respectively.

One of the merits of the FE model is that it allows a close monitoring of different variables of the capsule system which cannot be obtained from Matlab simulation or even be measured from experiment. Fig. 5 presents such variables as the functions of time by using the excitation parameters in Fig. 4(a). In Fig. 5(a), capsule's displacements in Y axis at different positions of the capsule are presented, where intestinal deformation at about 6.8 μm due to the capsule's

weight was recorded. Compared with the relative displacement between the magnet and the capsule in Fig. 5(c), it reveals that the capsule tilts up when their relative displacement increases, while moves down if the magnet reverses back to its original position, which can be demonstrated in the extra panels of Fig. 5(a). This tilted motion affects the distribution of the contact pressure between the capsule and the intestine as shown in Fig. 5(b) and its extra panels, so leading to a quasi-periodic intestinal friction on the capsule as presented in Fig. 5(d). This reason also explains the discrepancies observed in Fig. 4.

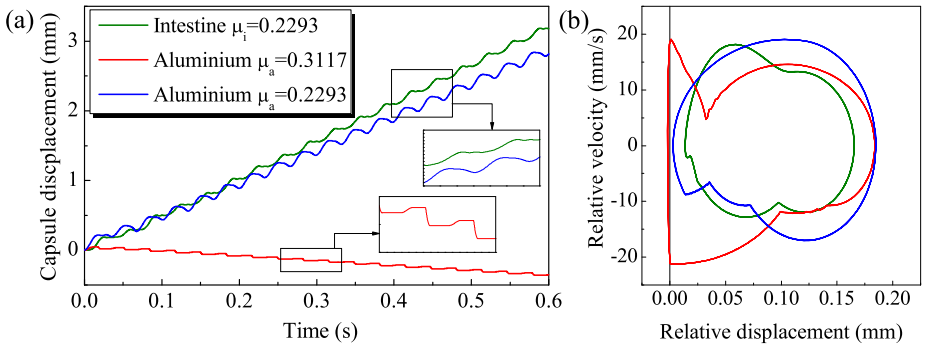

Fig. 6. (a) FE time histories of capsule's displacement in X axis and (b) phase trajectories obtained at the excitation frequency 30 Hz, the amplitude 6.8 mN, and the duty cycle 0.8. Green, red and blue lines represent the FE results obtained on the intestine ($\mu_{\mathrm{i}} = 0.2293$) and the aluminium bench ($\mu_{\mathrm{a}} = 0.3117$ and 0.2293), respectively. The vertical black line stands for the back impact boundary.

To further investigate the influence of the friction coefficient and intestinal deformation on the capsule, FE simulations under different friction coefficients and supporting substrates are compared in Fig. 6. Experimental identification of the friction coefficients was carried out by lifting one side of the supporting surface slowly until the stationary capsule started to move. So the friction coefficient was determined by the angle of the surface slope at that moment. It can be seen from Fig. 6(a) that although their friction coefficients were set the same, the capsule moved faster on the intestine as the intestinal deformation can prevent its backward motion at each period of excitation. While the capsule moving on the rigid aluminium bench had backward motion at each period of excitation. When the capsule moved on the aluminium bench with a larger friction coefficient ($\mu_{\mathrm{a}} = 0.3117$) measured from experiment, the capsule bifurcated from a period-one forward motion without any impact (at $\mu_{\mathrm{a}} = 0.2293$) to a period-one backward motion with one back impact. Such a qualitative change was due to the grazing-induced bifurcation as demonstrated in Fig. 6(b), where the capsule's phase trajectory crossed over the back impact boundary indicating the contact between the magnet and the secondary constraint.

To compare the tilted motion of the capsule on different substrates, Fig. 7 presents the maximum contact pressures on the substrates and its relevant in-

testinal frictions on the capsule. As can be seen from Fig. 7(a), the maximum contact pressure on the aluminium bench is much larger than the one on the intestine. This is due to the rigidity of the aluminium bench as illustrated in Fig. 8 such that when the capsule tilts up, it has much less contact area with the bench, while the intestine is "soft" resulting in a large contact area. Hence, such a difference in the supporting materials led to different frictions on the capsule.

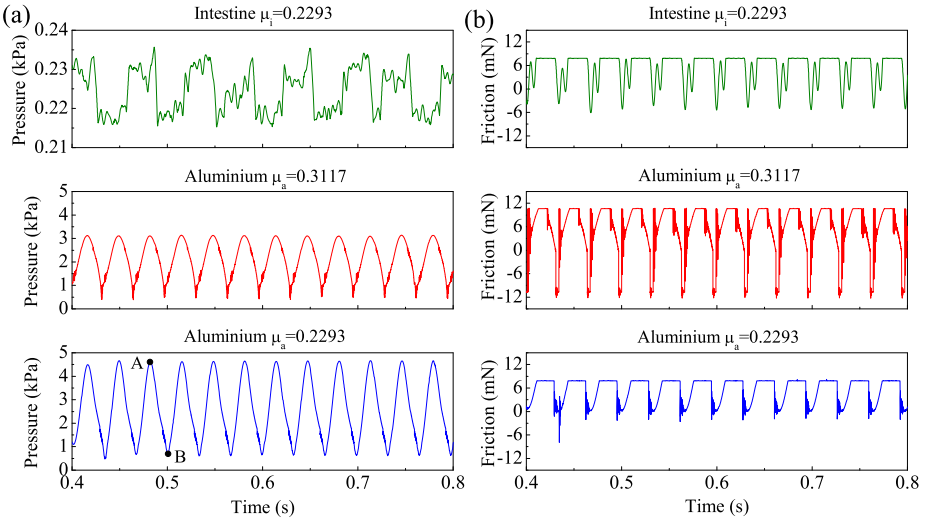

Fig. 7. (a) Maximum contact pressures and (b) intestinal frictions obtained at the excitation frequency 30 Hz, the amplitude 6.8 mN, and the duty cycle 0.8. Green, red and blue lines represent the FE results obtained on the intestine ($\mu_{\mathrm{i}} = 0.2293$) and the aluminium bench ($\mu_{\mathrm{a}} = 0.3117$ and 0.2293), respectively.

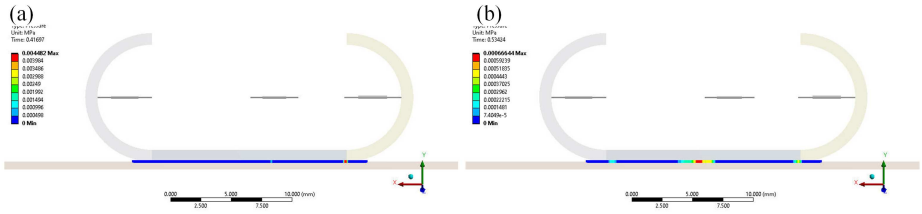

Fig. 8. The contour map of pressure distribution on the aluminium bench corresponding to points (a) A and (b) B marked in Fig. 7(a).

5 Conclusions

This paper studied a realistic 2D FE model to depict the nonlinear motion of the vibro-impact capsule moving on the small intestine. FE results were validated

using the simulation results obtained using non-smooth differential equations and the experimental results in [1]. Comparative analysis indicates that the FE model can better represent the capsule's dynamics and the contact with its substrate. It was found that the titled motion of the capsule during progression may cause asymmetric pressure on the substrate leading to quasi-periodic friction on the capsule. Therefore, a comprehensive bifurcation study for fully understanding its dynamics under intestinal peristalsis is recommended for future development.

Acknowledgement

This work has been supported by EPSRC under Grant No. EP/R043698/1. Mr Jiyuan Tian would like to acknowledge the financial support from the China Scholarship Council (award no. 201908060172) for his PhD scholarship.

References

1. Liu, Y., Páez Chávez, J., Zhang, J., Tian, J., Guo, B. and Prasad, S.: The vibro-impact capsule system in millimetre scale: numerical optimisation and experimental verification. Meccanica, to appear 1–18 (2020).
2. Guo, B., Liu, Y., Prasad, S.: Modelling of capsule–intestine contact for a self-propelled capsule robot via experimental and numerical investigation. Nonlinear Dynamics 98, 3155–3167 (2019).
3. Guo, B., Ley, E., Tian, J., Zhang, J., Liu, Y., Prasad, S.: Experimental and numerical studies of intestinal frictions for propulsive force optimisation of a vibro-impact capsule system. Nonlinear Dynamics 101, 65–83 (2020).
4. Yan, Y., Liu, Y., Manfredi, L., Prasad, S.: Modelling of a vibro-impact self-propelled capsule in the small intestine. Nonlinear Dynamics 96, 123–144 (2019).
5. Guo, B., Liu, Y., Birler, R., Prasad, S.: Self-propelled capsule endoscopy for small-bowel examination: proof-of-concept and model verification. International Journal of Mechanical Sciences 174, 105506 (2020).
6. Liu, Y., Páez Chávez, J., Guo, B., Birler, R.: Bifurcation analysis of a vibro-impact experimental rig with two-sided constraint. Meccanica, to appear 1-17 (2020).
7. Chernous'ko, F.L.: Two- and three-dimensional motions of a body controlled by an internal movable mass. Nonlinear Dynamics 99, 793–802 (2020).
8. Nunuparov, A., Becker, F., Bolotnik, N., Zeidis, I., Zimmermann, K.: Dynamics and motion control of a capsule robot with an opposing spring. Archive of Applied Mechanics 89, 2193–2208 (2019).
9. Glass, P., Cheung, E., Sitti, M.: A legged anchoring mechanism for capsule endoscopes using micropatterned adhesives. IEEE Transactions on Biomedical Engineering 55, 2759–2767 (2008).
10. Liu, Y., Pavlovskaia, E., Wiercigroch, M., Yu, H.: Modelling of a vibro-impact capsule system. International Journal of Mechanical Sciences 66, 2–11 (2013).
11. Zhan, X., Xu, J., Fang, H.: A vibration-driven planar locomotion robot — shell. Robotica 36, 1402–1420 (2018).
12. Liu, Y., Pavlovskaia, E., Wiercigroch, M., Peng, Z.: Forward and backward motion control of a vibro-impact capsule system. International Journal of Non-Linear Mechanics 70, 30–46 (2015).
13. Liu, Y., Pavlovskaia, E., Wiercigroch, M.: Experimental verification of the vibro-impact capsule model. Nonlinear Dynamics 83, 1029–1041 (2015).